Research Article Vol. 31, No. 21 / 9 Oct 2023 / Optics Express 35343
Optics EXPRESS

Impact of external carrier noise on the linewidth enhancement factor of a quantum dot distributed feedback laser

SHIHAO DING,[1,†] SHIYUAN ZHAO,[1,†] HEMING HUANG,[1] AND FRÉDÉRIC GRILLOT[1,2,*]

[1]LTCI, Télécom Paris, Institut Polytechnique de Paris, 19 Place Marguerite Perey, Palaiseau, 91120, France
[2]Center for High Technology Materials, University of New Mexico, 1313 Goddard St SE, Albuquerque, New Mexico 87106, USA
[†]These authors contributed equally to this paper
[*]frederic.grillot@telecom-paris.fr

Abstract: This paper demonstrates that the linewidth enhancement factor of quantum dot lasers is influenced by the external carrier transport issued from different external current sources. A model combining the rate equation and semi-classical carrier noise is used to investigate the different mechanisms leading to the above phenomenon in the context of a quantum dot distributed feedback laser. Meanwhile, the linewidth enhancement factor extracted from the optical phase modulation method shows dramatic differences when the quantum dot laser is driven by different noise-level pumps. Furthermore, the influence of external carrier noise on the frequency noise in the vicinity of the laser's threshold current directly affects the magnitude of the linewidth enhancement factor. Simulations also investigate how the external carrier transport impacts the frequency noise and the spectral linewidth of the QD laser. Overall, we believe that these results are of paramount importance for the development of on-chip integrated ultra-low noise oscillators producing light at or below the shot-noise level.

1. Introduction

Over the past decade, global Internet traffic has been exponentially increasing with the multiplication of end users [1]. Hyperscale data centers are widely deployed as pillars of the telecom infrastructure, supporting both individual and commercial usage, from where the optical transceivers became an essential part of the communication chain. At this stage, the phase noise is critical to high data rate throughput. The most common light source employed in optical transceivers are quantum well (QW) lasers, and these devices are not known for being low-phase noise oscillators, hence often exhibiting a typical optical linewidth on the order of a few MHz, which can not be directly exploited for the dense wavelength division multiplexing (DWDM) system application. On the other hand, intrinsic optical linewidth below 100 kHz has been widely reported in laser diodes made with quantum dot (QD) gain material [2–9]. Indeed, thanks to their three-dimensional carrier confinement and discrete distribution of the density of states, QD lasers, optical linewidths of QD lasers are about one order of magnitude smaller than their QW counterparts lasers, which is desirable for applications requiring advanced modulation formats [10], as well as for the development of novel transceivers based on subcarrier technology, for instance. In addition, QD lasers are compatible with both hybrid and epitaxial integration on silicon and exhibit low threshold current density, high thermal stability, and excellent optical feedback tolerance, making them ideal light source candidates for on-chip and short-reach optical links [11–15]. In recent years, QD lasers have been repeatedly reported as competent light sources for silicon-based photonic integrated circuits (PICs) [16–20], that are designed not only for optical transceivers but also for other advanced applications where low noise from the laser

#496131 https://doi.org/10.1364/OE.496131
Journal © 2023 Received 22 May 2023; revised 8 Sep 2023; accepted 29 Sep 2023; published 6 Oct 2023

Optics EXPRESS

source is imperative such as in chip-scale gyroscope and quantum cryptography, to name a few. In the telecom field, as the data traffic ramping-up is kept accelerating, scaling up transmission capacity is still necessary, therefore the utilization of low-cost kHz and sub-kHz local oscillators are required to leverage accessible 800 GBaud data rate [10,21]. For an integrated gyroscope, in order to make the most accurate rotational measurement devices, the light source needs to achieve low noise to improve the measurement accuracy for different scenarios [22]. Further, QD lasers have the potential to realize on-chip quantum key distribution (QKD). Last but not least, by exploiting the strong nonlinear properties of QD lasers, the quadrature amplitude of QD lasers can also be reduced below the standard quantum limit (SQL) to obtain amplitude-noise squeezing [23]. On these fronts, it is necessary to further suppress the noise level in QD lasers to deliver simple and low-cost on-chip options.

Against this backdrop, the α_H-factor is the key parameter to start with, since it quantifies the amplitude-phase fluctuation-coupling of semiconductor lasers under current injections, and is known to be a ruling aspect of not only the linewidth enhancement effects but also many other aspects of the laser such as the noise, the modulation, and nonlinear dynamics properties [24]. In the context of developing ultra-narrow line oscillators, it is relevant to investigate how the α_H-factor and subsequently the frequency noise is affected by the pumping conditions namely by the carrier transport across the junction [25]. The α_H-factor is conventionally expressed by the ratio between the refractive index and optical gain variations with respect to the carrier density [26], which acts as a fundamental basis for the noise performance. Typically, it has been demonstrated that the α_H-factor can be largely reduced using QD gain materials thanks to the energy quantization and the wave function confinement within the heterostructure potential in the three spatial dimensions [27]. The utilization of zero-dimensional nanostructures as active media has proved their abilities for reaching low-intensity and phase-noise oscillators [28]. Given that, it is important to better understand the role of the carrier noise generated from the current source in order to provide an additional way to further minimize the α_H-factor. Typically, a low noise current source (i.e. a quiet pump) is usually required to reduce the impact of external electrical noise when investigating the noise properties of a semiconductor laser [29–31]. Therefore, if one can transfer a constant carrier sequence into a quiet photon stream, then one would obtain sub-shot noise light. Fig. 1 illustrates the semiconductor laser pumped by a normal pump whereby electrons bunched, whereas the electrons are anti-bunched under a quiet pump for which the electrons stream does not show fluctuations in spacing, superior to the shot noise. This latter property directly transforms the photon distribution with sub-Poissonian statistics hence leading to the generation of non-classical states of light such as squeezed fields [32–34]. As a semiconductor laser is a combination of a resistor-capacitor and an inductor [35], it is important to better understand how the effects of the external carrier noise impact the electro-optical properties. Let us stress that prior works have deeply investigated the noise features from the laser junction but not really that from other circuit components like that from the current source [36]. These external noise sources greatly affect the behavior of injected carriers, which thus influences the laser-stimulated emission process.

In this paper, we investigate both numerically and experimentally the influence of external noise by considering the case of a distributed feedback (DFB) QD laser. The effects of carrier noise on the α_H-factor is usually analyzed by adding carrier, photon, and phase Langevin noise into a semi-classical model based on rate equations [37]. However, the carrier noise originating from the external current source is rarely considered in the literature [38,39], and even less for QD semiconductor lasers. Thereby, we implement the noise source and quiet current source conditions directly into our rate equation model. The α_H-factor is subsequently extracted from the frequency noise calculated by the diffusion coefficients. In addition to that, in our experiments, the effects of carrier transport are taken into account by considering two different current sources with distinct resistances. Previous studies indicated that semiconductor lasers exhibit different noise

Optics EXPRESS

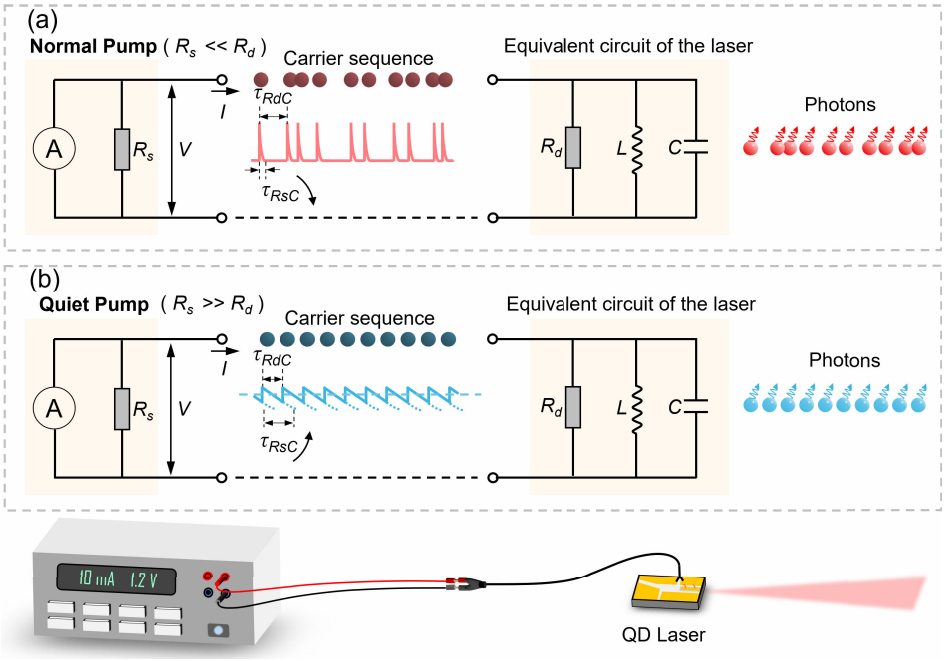

Fig. 1. Schematic diagram of the theoretical model illustrating the relationship between injected carriers and photons in a semiconductor laser driven by (a) a normal pump and (b) a quiet pump.

characteristics in such different bias conditions [32,40], which can definitely dwell tremendous repercussions on the physical properties of the QD laser such as the α_H-factor. Here, the α_H-factor is measured from around and above the laser threshold thanks to an optical phase modulation technique which does not introduce any underestimation of the α_H due to thermal effects. These results clearly indicate that the external carrier noise can affect the photon statistics, hence changing the linewidth enhancement effect, and subsequently the phase noise level. Therefore, we believe that this work releases consistent unique theoretical and experimental findings on the physics of QD lasers. Overall, the presented results can provide crucial guidelines for the development of ultra-low-noise oscillators for not only high throughput optical transceivers but also for other applications including Lidar systems, chip-scale gyroscopes, chemical and quantum sensing, where sub-kHz linewidth is often a prerequisite specification.

2. Theory and numerical model

Figure 1 shows two current pumps for the QD laser: (a) normal pump and (b) quiet pump. The effect of the pump on the laser is described with an equivalent circuit, where R_d is the junction differential resistance of the laser, L is the parasitic inductance, and C is the parasitic capacitance. The differential resistance emulates the damping resulting from the spontaneous and stimulated recombination terms in the rate equation. The inductance represents the resonance phenomenon of the laser. The capacitance contains the active layer diffusion capacitance and space charge capacitance of the laser [41,42]. The normal pump can be achieved practically when the laser junction differential resistance $R_d = (dI/dV)^{-1}$ is much larger than the internal resistance R_s of the pump whereas the quiet pump is obtained in the opposite limit. It should be emphasized that the current noise in semiconductor lasers is a combination of thermal diffusion noise and generation-recombination noise about the minority carrier. [43,44]. These noise events arise

Optics EXPRESS

sequentially and cause the departure of the minority carrier density from the equilibrium. Then, the external circuit would restore the steady-state distribution of minority carriers and regulate their injection into the active region via the relaxation process. For instance, when one has the normal pump with an infinitesimal source resistance R_s, this relaxation process would be completed with a negligible delay time $\tau_{R_sC} = R_sC$. As a result, the laser does not memorize the previous event and thus each event occurs independently from the statistical point of view, which is exactly the physical origin for the full-shot noise or photon Poissonian distribution as shown in Fig. 1(a). On the contrary, if one has a quiet pump with a considerable source resistance R_s, the modulation of minority carriers cannot be instantaneously eliminated by the external circuit because of a large time delay τ_{R_sC}. Therefore, the junction voltage is allowed to fluctuate by the thermal diffusive transit and generation-recombination events as shown in Fig. 1(b). In this context, if the recombination events exceed the average value, the junction voltage decreases due to the excess thermal diffusive transit. However, since this junction-voltage decrease is not recovered in time, the thermal diffusive transit rate temporarily decreases hence resulting in fewer recombination events. This sequence works as a self-feedback stabilization mechanism for regulating the pumping process, which potentially has a significant impact on the α_H-factor and the noise spectrum.

A quiet pump with a sub-Poissonian carrier distribution and a normal pump with a Gaussian carrier distribution can be well described by using a stochastic model [34,45]. However, in this kind of representation, the inclusion of the phase term influencing the α_H-factor is rather complicated. Instead, the frequency noise and the α_H-factor of a QD laser can be better modeled with a rate equation approach [46,47]. Here, we incorporate into these rate equations the various noise contributions by taking into account the different current sources. As shown in Fig. 2, the QD carrier dynamics is described by considering a three-energy level system. The model assumes a single-mode emission which is exactly the configuration achieved with the QD DFB laser under study. Besides, it holds under the assumption that the active region consists of only one QD ensemble, where the nanostructures are interconnected by a two-dimensional reservoir state (RS) [48]. The QD contains two bound states: a two-fold degenerate ground state (GS) and a four-fold degenerate excited state (ES). QDs are implicitly assumed to be always neutral, electrons and holes are treated as electron-hole pairs, which means that the system is only composed of excitonic energy states. Carriers are supposed to be injected directly from the contacts into the RS levels. When different pumps set the same current, it can be assumed that the current expected value is the same, but the variance is different. The different variances represent different noise levels. The coupled rate equations on carrier, phase, and photon dynamics read as follows:

$$\frac{dN_{RS}}{dt} = \frac{\eta I}{q} + \frac{N_{ES}}{\tau_{RS}^{ES}} - \frac{N_{RS}}{\tau_{ES}^{RS}}(1-\rho_{ES}) - \frac{N_{RS}}{\tau_{RS}^{spon}} + F_{RS} \tag{1}$$

$$\frac{dN_{ES}}{dt} = (\frac{N_{RS}}{\tau_{ES}^{RS}} + \frac{N_{GS}}{\tau_{ES}^{GS}})(1-\rho_{ES}) - \frac{N_{ES}}{\tau_{GS}^{ES}}(1-\rho_{GS}) - \frac{N_{ES}}{\tau_{RS}^{ES}} - \frac{N_{ES}}{\tau_{ES}^{spon}} + F_{ES} \tag{2}$$

$$\frac{dN_{GS}}{dt} = \frac{N_{ES}}{\tau_{GS}^{ES}}(1-\rho_{GS}) - \frac{N_{GS}}{\tau_{ES}^{GS}}(1-\rho_{ES}) - \Gamma_p v_g g_{GS} S_{GS} - \frac{N_{GS}}{\tau_{GS}^{spon}} + F_{GS} \tag{3}$$

$$\frac{dS_{GS}}{dt} = (\Gamma_p v_g g_{GS} - \frac{1}{\tau_p})S_{GS} - \beta_{SP}\frac{N_{GS}}{\tau_{GS}^{spon}} + F_S \tag{4}$$

$$\frac{d\phi}{dt} = \Delta\omega_N^{GS} + \Delta\omega_N^{ES} + \Delta\omega_N^{RS} + F_\phi \tag{5}$$

where the carrier numbers in the GS, ES, and RS energy levels are denoted by N_{RS}, N_{ES}, and N_{GS} respectively while S_{GS} is the photon number in the GS and ϕ accounts for the phase of

Optics EXPRESS

the electrical field. The carrier dynamics are shortly described as follows. First, carriers are captured from the RS to the ES with a capture time τ_{ES}^{RS} then they relax from the ES down to the GS level with a relaxation time τ_{GS}^{ES}. Carriers can also be thermally re-emitted from the ES to the RS with an escape time τ_{RS}^{ES}. Similar dynamic behavior is followed for the carrier population on the GS level with regard to the ES. In addition, carriers can also recombine spontaneously with spontaneous emission times τ_{RS}^{spon}, τ_{ES}^{spon}, and τ_{GS}^{spon} at RS, ES, and GS levels, respectively. As shown in Eq. (1), the pumping term $\eta I/q$ incorporates the injection efficiency η and q the elementary charge. Lastly, it should be pointed out that ρ_{ES}, ρ_{GS} correspond to the carrier occupation probabilities into the ES and GS while β_{sp} is the fraction of the spontaneous emission coupled in the lasing mode, Γ_p is the optical confinement factor, v_g is the group velocity and $\Delta\omega_N^{RS,ES,GS}$ accounts for the frequency shift of the carrier-induced laser field relative to the frequency. $F_{RS,ES,GS,S,\phi}$ are the Langevin noise terms. The materials and optical parameters used in the simulations are placed in Supplement 1. The characteristics of the QD laser are investigated by small signal analysis.

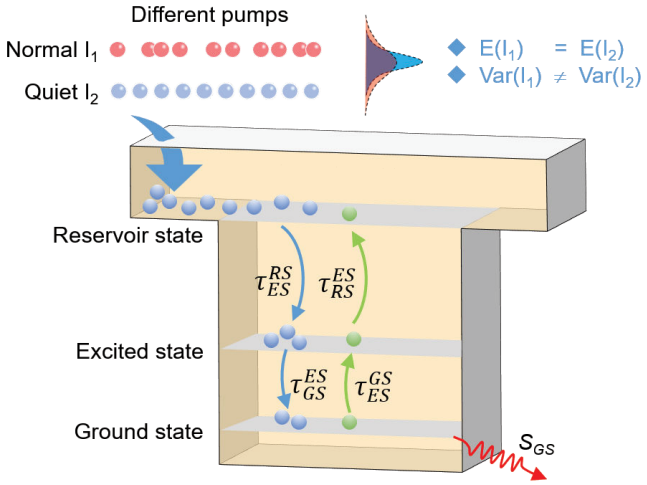

Fig. 2. Schematic representation of the electronic structure and carrier dynamics in a QD for normal pumping conditions and quiet pumping conditions.

By using the Langevin approach, we investigate the characteristics of the frequency noise, where the different carrier noises imposed by different current sources will be reflected. We introduce $F_{RS}(t)$, $F_{ES}(t)$, $F_{GS}(t)$, $F_S(t)$, and $F_\phi(t)$ as Langevin noise terms into the carrier, photon, and phase rate equations. Moreover, the correlation strength of noise sources is $<F_i(t)\,F_j(t)>$ $= 2D_{i-j}\delta(t-t')$, where indexes i, j refer to N_{RS}, N_{ES}, N_{GS}, S, and Φ where D_{i-j} is the diffusion coefficient between two noise sources that are delta correlated. Fig. 3 briefly explains to the reservoir model in order to characterize the laser noise performance. Pumped carriers are injected into the laser structure (I/q), of which only a certain fraction $(\eta I/q)$ arrive in the active region. We considered carrier noise fluctuations on sub-nanosecond time scales since carrier noise remains distinguishable at frequencies higher than GHz. At this point the carrier noise time scale coincides with carrier lifetimes and photon lifetimes of almost one order of magnitude, so the diffusion coefficient between the two noise sources is delta-correlated [49]. Then, some carriers participate in the spontaneous emission, and others go to the ES energy level and participate in the subsequent dynamical processes. After the process of spontaneous and stimulated emission of ES, some of the carriers reach the GS energy level. Finally, let us stress that the QD laser under study only emits on the GS transition therefore the stimulated emission in ES is not considered.

Optics EXPRESS

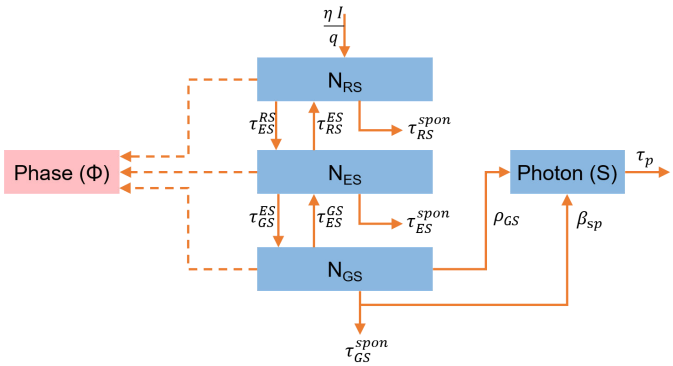

Fig. 3. Reservoir model used in the rate equation analysis of the QD laser. Each solid line arrow in the flow chart represents the number of particles flowing per unit of time. The dashed lines represent the relationship to the phase.

After the analysis of the particle flows into/out of the different reservoirs using the method described in [50,51], the diffusion coefficients can be derived as follows. This would be the critical aspect of distinguishing the different carrier noises from different sources.

$$D_{R-R} = \frac{\eta I}{q} + \frac{N_{ES}}{\tau_{RS}^{ES}} + \frac{N_{RS}}{\tau_{ES}^{RS}}(1-\rho_{ES}) + \frac{N_{RS}}{\tau_{RS}^{spon}} \tag{6}$$

$$D_{E-E} = (\frac{N_{RS}}{\tau_{ES}^{RS}} + \frac{N_{GS}}{\tau_{ES}^{GS}})(1-\rho_{ES}) + \frac{N_{ES}}{\tau_{GS}^{ES}}(1-\rho_{GS}) + \frac{N_{ES}}{\tau_{RS}^{ES}} + \frac{N_{ES}}{\tau_{ES}^{spon}} \tag{7}$$

$$D_{G-G} = \frac{N_{ES}}{\tau_{GS}^{ES}}(1-\rho_{GS}) + \frac{N_{GS}}{\tau_{ES}^{GS}}(1-\rho_{ES}) + \Gamma_p v_g g_{GS} S_{GS} + \frac{N_{GS}}{\tau_{GS}^{spon}} \tag{8}$$

$$D_{S-S} = (\Gamma_p v_g g_{GS} - \frac{1}{\tau_p}) S_{GS} + \beta_{SP} \frac{N_{GS}}{\tau_{GS}^{spon}} \tag{9}$$

$$D_{\phi-\phi} = \Delta\omega_N^{GS} + \Delta\omega_N^{ES} + \Delta\omega_N^{RS} \tag{10}$$

$$D_{R-E} = -\left[\frac{N_{RS}}{\tau_{ES}^{RS}}(1-\rho_{ES}) + \frac{N_{ES}}{\tau_{RS}^{ES}}\right] \tag{11}$$

$$D_{E-G} = -\left[\frac{N_{GS}}{\tau_{ES}^{GS}}(1-\rho_{ES}) + \frac{N_{ES}}{\tau_{GS}^{ES}}(1-\rho_{GS})\right] \tag{12}$$

$$D_{G-S} = -\left[\beta_{SP}\frac{N_{GS}}{\tau_{GS}^{spon}} + \Gamma_p v_g g_{GS} S_{GS}\right] \tag{13}$$

$$D_{R-G} = D_{R-S} = D_{R-\phi} = D_{E-S} = D_{E-\phi} = D_{G-\phi} = D_{S-\phi} = 0 \tag{14}$$

Optics EXPRESS

Following Cramer's rule [52] and the above diffusion coefficients, the frequency noise (FN) of the QD laser can be expressed by Eq. (15).

$$\begin{aligned} FN(\omega) = \left\langle \left| \frac{j\omega}{2\pi}\delta\phi(\omega) \right|^2 \right\rangle = \left\langle \left| j\omega \frac{\Delta_\phi}{\Delta} \right|^2 \right\rangle = \frac{\omega^2}{\Delta^2} \Big\{ \left\langle |D_{R-R}|^2 \right\rangle |M_{R-\phi}|^2 + \left\langle |D_{E-E}|^2 \right\rangle |M_{E-\phi}|^2 \\ + \left\langle |D_{G-G}|^2 \right\rangle |M_{G-\phi}|^2 + \left\langle |D_{S-S}|^2 \right\rangle |M_{S-\phi}|^2 + \left\langle |D_{\phi-\phi}|^2 \right\rangle |M_{\phi-\phi}|^2 \\ -2 \left\langle D_{R-E} D^*_{R-E} \right\rangle Re(M_{R-\phi} M^*_{E-\phi}) - 2 \left\langle D_{E-G} D^*_{E-G} \right\rangle Re(M_{E-\phi} M^*_{G-\phi}) \\ -2 \left\langle D_{G-S} D^*_{G-S} \right\rangle Re(M_{G-\phi} M^*_{S-\phi}) \Big\} \end{aligned} \tag{15}$$

where ω is the angular frequency applied on the QD laser. The M_{i-j} are the algebraic cofactors of Δ_ϕ. Δ is the determinant obtained from the system of Eqs. (1-5).

3. Results and discussion

The diffusion coefficient D_{R-R} serves as our key parameter for correlating frequency noise and current source noise. When using a normal pump to drive the laser, we consider that the current noise term $\eta I/q$ affects the QD laser through the reservoir state into the active medium. When injecting a quiet current to the QD laser, we can remove the $\eta I/q$ from the D_{R-R} and thus assume that the current is noise-free for the QD laser. According to the above theory and Eq. (15), the FN curves are obtained under different current sources as shown in Fig. 4(a-d). As the current increases, the frequency noise issued from the two current sources gradually approaches the low-frequency plateau. The FN value at low frequency corresponds to the optical linewidth ($\Delta\nu_{OL}$) of the QD laser, while that at the high-frequency plateau gives the Schawlow-Townes linewidth ($\Delta\nu_{ST}$). It can be seen that the FN's response at high-frequency does not depend on the current sources. In other words, whatever normal pump or quiet pump, it has no effect on the spontaneous emission noise dominated by the characteristics of the gain medium. The peak between the two plateaus arising above the threshold current corresponds to the relaxation oscillation frequency (F_{RO}) of the QD laser. To this end, when the frequency is lower than F_{RO}, the FN is determined not only by the spontaneous emission but also by the carrier fluctuations, and the optical linewidth can be expressed as $\Delta\nu_{OL} = \Delta\nu_{ST}(1+\alpha_H^2)$. Therefore, as the optical linewidth is driven by different carrier noises, the linewidth enhancement factor is influenced. In addition, maps displayed in Fig. 4(e) and 4(f) show that when the laser operates with a quiet pump, the FN exhibits superior levels around the threshold transition. The inflection point at the resonance frequency near 1.8 times threshold is attributed to the spontaneous emission factor ($\beta_{sp} = 1\times 10^{-4}$). Due to the limited spontaneous emission efficiency, the laser output power has a nonlinear relationship with the above-threshold current. Overall, these simulations unlock how the carrier noise originating from the current source impacts the FN of the QD laser in particular near the threshold transition.

In the following, the α_H-factor is extracted from the FN simulations and compared to the experiments for different current source conditions. The two pumps were experimentally measured to exhibit different noise characteristics. The specific methods and results are described in the Supplement 1. To do so, a commercial QD DFB laser is used to extract the α_H-factor around and above the threshold current using an optical phase modulation method. The modulation of the QD DFB laser at high frequency (13 ~ 18 GHz) leads to distinct side modes in the optical spectrum and the side modes at different optical delays are used to retrieve the α_H-factor. The experiment is performed at room temperature (20 °C). Further details can be found in Supplement 1 and in the references [53,54]. Such an approach allows us to retrieve the pump current dependence of the α_H-factor with and without quiet conditions. Experimental results are depicted in Fig. 5(a) and compared with simulations (solid lines). Near the threshold current, it is shown that the

Optics EXPRESS

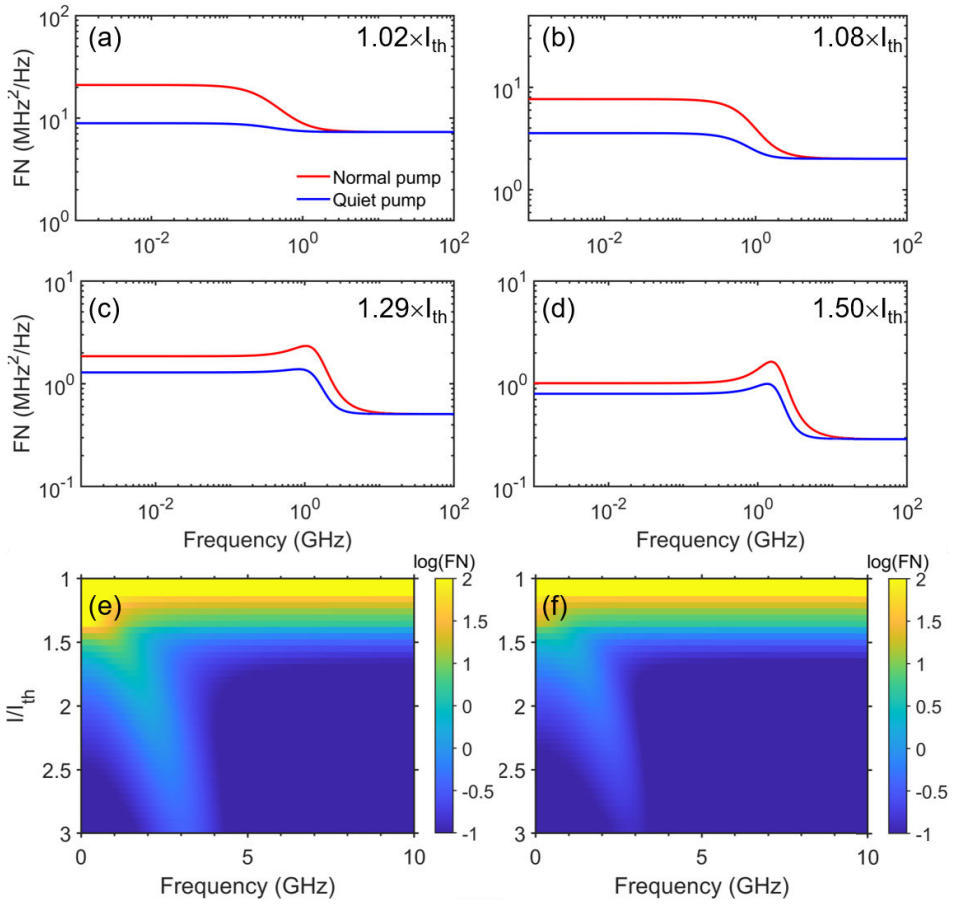

Fig. 4. Simulated frequency noise spectra of the QD laser with normal pump (red line) and quiet pump (blue line) at different bias currents (a-d). The frequency noise mapping with bias pump and frequency under (e) normal pump and (f) quiet pump.

α_H-factor becomes much smaller under quiet pumping conditions. For instance at the threshold, with a normal pump, the α_H-factor is about 1.7 while it is reduced to 0.5 with quiet pumping. To generate this different carrier noise in the numerical model, we set $\eta I/q$ to 0 for the quiet pump case and set the actual current as a normal pump because the $\eta I/q$ is the external carrier noise source. The louder the carrier noise, the easier it is to be captured by defect states and to affect the efficiency of the stimulated emission. Simulations also reveal that near the threshold transition, the α_H-factor balloons as shown in the red curve in Fig. 5(a) which is due to a combination of population inversion and inefficient emission by carrier noise. Indeed, the optical phase modulation requires sufficient power from the laser which is hardly the case when operating near the threshold. Despite that, we demonstrate that the measured α_H-factors are qualitatively in good agreement with those from the simulations. Interestingly, previous work also showed a rise of the α_H-factor extracted in a QD laser from amplified spontaneous emission (ASE) and normal pump across the threshold, but the exact reasons for this phenomenon remain unclear [27]. Whereas, with the quiet carriers driving, the α_H-factor of the QD laser near threshold current only appears as a step due to population inversion, which was also simulated in the reference [25]. The α_H-factor doesn't drop to zero at sub-threshold but approximates a minute value of approximately 0.02. Even when the effect of external carrier noise was eliminated in

Optics EXPRESS

quiet pumping simulations, the impacts of spontaneous emission and other intrinsic noises on the sub-threshold α_H-factor remain, leading to a diminished α_H-factor value that is not entirely zero. Furthermore, both our experimental and simulation results show that no more differences are observed as the current increases. The α_H-factor becomes independent of the carrier noise.

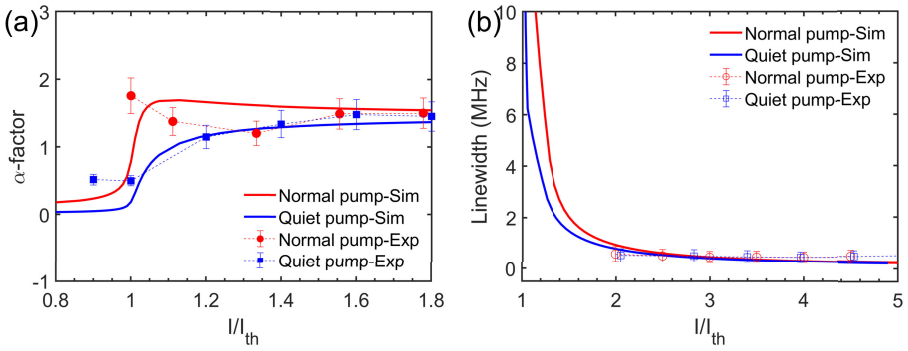

Fig. 5. Experimental (dotted line) and simulated (solid line) (a) α_H-factor and (b) optical linewidth with bias current under different pumps.

As the optical linewidth is linked to the α_H-factor, the measurement of the QD DFB laser's linewidth is also performed with a delayed self-heterodyne interferometer at 20 °C. Results are shown by the dots in Fig. 5(b) for both normal and quiet pump conditions. In order to extract the linewidths, a Voigt fitting profile is used. Due to technical limitations on the coupled output power, the optical linewidths could only be extracted above twice the threshold current. As expected, we found that the linewidth evolves with the injection current with a sharp decrease above the threshold from several MHz down to a stable value of approximately 500 kHz which is typical for a QD laser [2]. At high pump current, there is no significant difference in the optical linewidth when driven by different current sources, which is also consistent with the simulation results. However, when the laser is driven slightly above the threshold, simulations reveal that the use of a normal pump only contributes to increasing the linewidth. For instance, at 1.5 times the threshold current, the optical linewidth is 1.8 MHz when the quiet pump is against 3.2 MHz for the normal pumping conditions. The α_H-factor obtained under different noise conditions of the pump directly determines the tendency of the linewidth. The linewidth will be expanded in a squared α_H-factor manner. The overlap of α_H-factor at high currents also makes the linewidth independent of different noise conditions pump. Therefore, the impacts of external carrier noise on frequency noise dramatically extend to both the α_H-factor and the optical linewidth.

4. Conclusion

This work investigates the influence of the external carrier transport on the α_H-factor of a QD DFB laser. With the quiet pump, the α_H-factor is found to be much smaller around the threshold as compared to normal pump conditions. Numerical models and experiments together verify this interesting phenomenon. On top of that, simulations also highlight that the use of the quiet pump near the threshold current is beneficial for reducing the frequency noise and subsequently the optical linewidth, but has less impact at high currents. It must be emphasized that the α_H-factor of the QW laser under different pumps described in Supplement 1 also demonstrates similar results to those of the QD laser. Future work will concentrate on the generation of squeezed states for producing low-noise QD lasers below or at the shot noise level.

Funding. Air Force Office of Scientific Research (A8655-23-1-7050); Institut Mines-Télécom; China Scholarship Council.

Optics EXPRESS

Acknowledgments. The authors acknowledge the financial support of the Institut Mines-Télécom and the Air Force Office of Scientific Research (AFSOR). Shihao Ding's work is also supported by the China Scholarship Council (CSC). Special thanks to Prof. Dr. W. Elsaesser from TU Darmstadt, Germany, for fruitful discussions.

Disclosures. The authors declare no conflicts of interest.

Data Availability. Data underlying the results presented in this paper are not publicly available at this time but may be obtained from the authors upon reasonable request.

Supplemental document. See Supplement 1 for supporting content.

References

1. G. Kamiya, "Data Centres and Data Transmission Networks," Tech. rep., International Energy Agency (2021).
2. H. Su and L. F. Lester, "Dynamic properties of quantum dot distributed feedback lasers: high speed, linewidth and chirp," J. Phys. D: Appl. Phys. **38**(13), 2112–2118 (2005).
3. Z. G. Lu, P. J. Poole, J. R. Liu, P. J. Barrios, Z. J. Jiao, G. Pakulski, D. Poitras, D. Goodchild, B. Rioux, and A. J. SpringThorpe, "High-performance 1.52 μm InAs/InP quantum dot distributed feedback laser," Electron. Lett. **47**(14), 818–819 (2011).
4. M. T. Crowley, N. A. Naderi, H. Su, F. Grillot, and L. F. Lester, "GaAs-based quantum dot lasers," in *Semiconductors and Semimetals*, vol. 86 (Elsevier, 2012), pp. 371–417.
5. G. Eisenstein and D. Bimberg, *Green Photonics and Electronics* (Springer, 2017).
6. A. Becker, V. Sichkovskyi, M. Bjelica, A. Rippien, F. Schnabel, M. Kaiser, O. Eyal, B. Witzigmann, G. Eisenstein, and J. P. Reithmaier, "Widely tunable narrow-linewidth 1.5 μm light source based on a monolithically integrated quantum dot laser array," Appl. Phys. Lett. **110**(18), 181103 (2017).
7. C. Redlich, B. Lingnau, H. Huang, R. Raghunathan, K. Schires, P. Poole, F. Grillot, and K. Lüdge, "Linewidth rebroadening in quantum dot semiconductor lasers," IEEE J. Sel. Top. Quantum Electron. **23**(6), 1–10 (2017).
8. J. Duan, H. Huang, Z. Lu, P. Poole, C. Wang, and F. Grillot, "Narrow spectral linewidth in inas/inp quantum dot distributed feedback lasers," Appl. Phys. Lett. **112**(12), 121102 (2018).
9. Y. Wan, C. Xiang, and J. Guo, *et al.*, "High speed evanescent quantum-dot lasers on si," Laser Photonics Rev. **15**, 2100057 (2021).
10. M. Seimetz, "Laser Linewidth Limitations for Optical Systems with High-Order Modulation Employing Feed Forward Digital Carrier Phase Estimation," in *OFC/NFOEC 2008 - 2008 Conference on Optical Fiber Communication/National Fiber Optic Engineers Conference*, (2008), pp. 1–3.
11. K. Mizutani, K. Yashiki, M. Kurihara, Y. Suzuki, Y. Hagihara, N. Hatori, T. Shimizu, Y. Urino, T. Nakamura, K. Kurata, and Y. Arakawa, "Isolator free optical I/O core transmitter by using quantum dot laser," in *2015 IEEE 12th International Conference on Group IV Photonics (GFP)*, (IEEE, 2015), pp. 177–178.
12. J. Duan, H. Huang, B. Dong, D. Jung, J. C. Norman, J. E. Bowers, and F. Grillot, "1.3-μm reflection insensitive inas/gaas quantum dot lasers directly grown on silicon," IEEE Photonics Technol. Lett. **31**(5), 345–348 (2019).
13. J. C. Norman, D. Jung, Y. Wan, and J. E. Bowers, "Perspective: The future of quantum dot photonic integrated circuits," APL Photonics **3**(3), 030901 (2018).
14. Y. Arakawa, T. Nakamura, and J. Kwoen, "Chapter Three - Quantum dot lasers for silicon photonics," in *Future Directions in Silicon Photonics*, vol. 101 of *Semiconductors and Semimetals* S. Lourdudoss, J. E. Bowers, and C. Jagadish, eds. (Elsevier, 2019), pp. 91–138.
15. Z. Yan, Y. Han, L. Lin, Y. Xue, C. Ma, W. K. Ng, K. S. Wong, and K. M. Lau, "A monolithic InP/SOI platform for integrated photonics," Light: Sci. Appl. **10**(1), 200 (2021).
16. Y. Arakawa, T. Nakamura, and K. Kurata, "Highlights of 10-years of Research in a Japanese Si Photonics Project," in *2022 Optical Fiber Communications Conference and Exhibition (OFC)*, (2022), pp. 1–4.
17. D. Jung, Z. Zhang, and J. Norman, *et al.*, "Highly reliable low-threshold inas quantum dot lasers on on-axis (001) si with 87% injection efficiency," ACS Photonics **5**(3), 1094–1100 (2018).
18. F. Grillot, J. C. Norman, J. Duan, Z. Zhang, B. Dong, H. Huang, W. W. Chow, and J. E. Bowers, "Physics and applications of quantum dot lasers for silicon photonics," Nanophotonics **9**(6), 1271–1286 (2020).
19. Tower Semiconductor, "Tower Semiconductor Announces World's First Heterogeneous Integration of Quantum Dot Lasers on its Popular SiPho Foundry Platform PH18," (2023).
20. K. Kurata, "AIO Core Announces Industry's first Quantum Dot Laser based Silicon Photonics Transceiver chips for 32Gbps PCIe Gen 5," in *2023 Optical Fiber Communications Conference and Exhibition (OFC)*, (2023).
21. W. Shi, Y. Tian, and A. Gervais, "Scaling capacity of fiber-optic transmission systems via silicon photonics," Nanophotonics **9**(16), 4629–4663 (2020).
22. Y.-H. Lai, M.-G. Suh, Y.-K. Lu, B. Shen, Q.-F. Yang, H. Wang, J. Li, S. H. Lee, K. Y. Yang, and K. Vahala, "Earth rotation measured by a chip-scale ring laser gyroscope," Nat. Photonics **14**(6), 345–349 (2020).
23. G. Moody, L. Chang, T. J. Steiner, and J. E. Bowers, "Chip-scale nonlinear photonics for quantum light generation," AVS Quantum Sci. **2**(4), 041702 (2020).
24. K. Lüdge and H. Schuster, *Nonlinear Laser Dynamics: From Quantum Dots to Cryptography*, Reviews of Nonlinear Dynamics and Complexity (Wiley, 2012).
25. S. Melnik, G. Huyet, and A. V. Uskov, "The linewidth enhancement factor α of quantum dot semiconductor lasers," Opt. Express **14**(7), 2950–2955 (2006).

Optics EXPRESS

26. C. Henry, "Theory of the linewidth of semiconductor lasers," IEEE J. Quantum Electron. **18**(2), 259–264 (1982).
27. J. Duan, H. Huang, D. Jung, Z. Zhang, J. Norman, J. Bowers, and F. Grillot, "Semiconductor quantum dot lasers epitaxially grown on silicon with low linewidth enhancement factor," Appl. Phys. Lett. **112**(25), 251111 (2018).
28. P. Yu and Z. Wang, *Quantum Dot Optoelectronic Devices*, Lecture Notes in Nanoscale Science and Technology (Springer International Publishing, 2020).
29. A. Malik, C. Xiang, L. Chang, W. Jin, J. Guo, M. Tran, and J. Bowers, "Low noise, tunable silicon photonic lasers," Appl. Phys. Rev. **8**(3), 031306 (2021).
30. S. Bartalini, S. Borri, P. Cancio, A. Castrillo, I. Galli, G. Giusfredi, D. Mazzotti, L. Gianfrani, and P. De Natale, "Observing the intrinsic linewidth of a quantum-cascade laser: beyond the schawlow-townes limit," Phys. Rev. Lett. **104**(8), 083904 (2010).
31. S. Liu, X. Wu, D. Jung, J. C. Norman, M. Kennedy, H. K. Tsang, A. C. Gossard, and J. E. Bowers, "High-channel-count 20 ghz passively mode-locked quantum dot laser directly grown on si with 4.1 tbit/s transmission capacity," Optica **6**(2), 128–134 (2019).
32. S. Machida, Y. Yamamoto, and Y. Itaya, "Observation of amplitude squeezing in a constant-current–driven semiconductor laser," Phys. Rev. Lett. **58**(10), 1000–1003 (1987).
33. J. Mork and G. Lippi, "Rate equation description of quantum noise in nanolasers with few emitters," Appl. Phys. Lett. **112**(14), 141103 (2018).
34. J. Mork and K. Yvind, "Squeezing of intensity noise in nanolasers and nanoleds with extreme dielectric confinement," Optica **7**(11), 1641–1644 (2020).
35. J. Kim, S. Somani, and Y. Yamamoto, *Nonclassical light from semiconductor lasers and LEDs*, vol. 5 (Springer Science & Business Media, 2012).
36. J.-L. Vey and P. Gallion, "Semiclassical model of semiconductor laser noise and amplitude noise squeezing. i. description and application to fabry-perot laser," IEEE J. Quantum Electron. **33**(11), 2097–2104 (1997).
37. J. Duan, X.-G. Wang, Y.-G. Zhou, C. Wang, and F. Grillot, "Carrier-noise-enhanced relative intensity noise of quantum dot lasers," IEEE J. Quantum Electron. **54**(6), 1–7 (2018).
38. J. Arnaud, "Classical theory of laser noise," Optical and Quantum Electronics **27**(2), 63–89 (1995).
39. J. Arnaud, "Detuned inhomogeneously broadened laser linewidth," Quantum Semiclass. Opt. **9**(4), 507–518 (1997).
40. S. Machida and Y. Yamamoto, "Ultrabroadband amplitude squeezing in a semiconductor laser," Phys. Rev. Lett. **60**(9), 792–794 (1988).
41. R. Tucker and D. Pope, "Circuit modeling of the effect of diffusion on damping in a narrow-stripe semiconductor laser," IEEE J. Quantum Electron. **19**(7), 1179–1183 (1983).
42. R. Tucker and D. J. Pope, "Microwave circuit models of semiconductor injection lasers," IEEE Trans. Microwave Theory Techn. **31**(3), 289–294 (1983).
43. Y. Yamamoto, S. Machida, and O. Nilsson, "Amplitude squeezing in a pump-noise-suppressed laser oscillator," Phys. Rev. A **34**(5), 4025–4042 (1986).
44. Y. Yamamoto and H. A. Haus, "Effect of electrical partition noise on squeezing in semiconductor lasers," Phys. Rev. A **45**(9), 6596–6604 (1992).
45. S. Zhao and F. Grillot, "Stochastic model of sub-poissonian quantum light in an interband cascade laser," Phys. Rev. Appl. **18**(6), 064027 (2022).
46. C. Wang, B. Lingnau, K. Lüdge, J. Even, and F. Grillot, "Enhanced dynamic performance of quantum dot semiconductor lasers operating on the excited state," IEEE J. Quantum Electron. **50**(9), 1–9 (2014).
47. Y. Zhou, J. Duan, F. Grillot, and C. Wang, "Optical noise of dual-state lasing quantum dot lasers," IEEE J. Quantum Electron. **56**(6), 1–7 (2020).
48. C. Wang, J.-P. Zhuang, F. Grillot, and S.-C. Chan, "Contribution of off-resonant states to the phase noise of quantum dot lasers," Opt. Express **24**(26), 29872–29881 (2016).
49. G. P. Agrawal and R. Roy, "Effect of injection-current fluctuations on the spectral linewidth of semiconductor lasers," Phys. Rev. A **37**(7), 2495–2501 (1988).
50. L. A. Coldren, S. W. Corzine, and M. L. Mashanovitch, *Diode lasers and photonic integrated circuits* (John Wiley & Sons, 2012).
51. S. Zhao and F. Grillot, "Modeling of amplitude squeezing in a pump-noise-suppressed interband cascade laser," IEEE Photonics J. **14**(3), 1–8 (2022).
52. D. McCumber, "Intensity fluctuations in the output of cw laser oscillators. i," Phys. Rev. **141**(1), 306–322 (1966).
53. B. Dong, J. Duan, H. Huang, J. C. Norman, K. Nishi, K. Takemasa, M. Sugawara, J. E. Bowers, and F. Grillot, "Dynamic performance and reflection sensitivity of quantum dot distributed feedback lasers with large optical mismatch," Photonics Res. **9**(8), 1550–1558 (2021).
54. S. Ding, B. Dong, H. Huang, J. Bowers, and F. Grillot, "Spectral dispersion of the linewidth enhancement factor and four wave mixing conversion efficiency of an inas/gaas multimode quantum dot laser," Appl. Phys. Lett. **120**(8), 081105 (2022).